Bioconjugate Chemistry

Article

pubs.acs.org/bc

Bioconjugation of Gold Nanoparticles through the Oxidative Coupling of *ortho*-Aminophenols and Anilines

Stacy L. Capehart,[†,‡] Adel M. ElSohly,[†] Allie C. Obermeyer,[†] and Matthew B. Francis*[,†,‡]

[†]Department of Chemistry, University of California, Berkeley, Berkeley, California 94720, United States

[‡]Materials Sciences Division, Lawrence Berkeley National Laboratories, Berkeley, California 94720-1460, United States

Supporting Information

ABSTRACT: While there are a number of methods for attaching gold nanoparticles (AuNPs) to biomolecules, the existing strategies suffer from nonspecific AuNP adsorption, reagents that are unstable in aqueous solutions, and/or long reaction times. To improve upon existing AuNP bioconjugation strategies, we have adapted a recently reported potassium ferricyanide-mediated oxidative coupling reaction for the attachment of aniline-functionalized AuNPs to *o*-aminophenol-containing oligonucleotides, peptides, and proteins. The aniline-AuNPs are stable in aqueous solutions, show little-to-no nonspecific adsorption with biomolecules, and react rapidly (30 min) with *o*-aminophenols under mild conditions (pH 6.5, 1 mM oxidant).

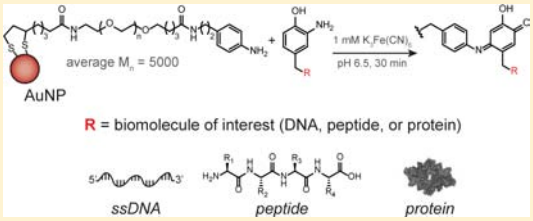

INTRODUCTION

The specific conjugation of AuNPs to biomolecules has applications in imaging,[1,2] drug delivery,[3] and enzyme immobilization.[4−7] As a result, a number of existing strategies have been developed for the covalent attachment of gold nanoparticles (AuNPs) to biomolecules.[8−11] Most commonly, these approaches take advantage of the strong thiol−AuNP interactions (~200 kJ/mol in bond energy),[12] allowing cysteine-containing peptides,[13−15] thiol-DNA,[16] and proteins with solvent accessible cysteines[17,18] to be attached to AuNPs. Proteins have also been adsorbed to negatively charged AuNPs through electrostatic interactions.[19,20] Affinity-based, noncovalent interactions, such as the biotin−streptavidin interaction,[4,21] and the His_6/nickel−nitrilotriacetic acid (NTA) interaction,[11,22,23] have also been used to produce AuNP−protein conjugates. Furthermore, the covalent conjugation of proteins to suitably functionalized AuNPs has been demonstrated using EDC/NHS activation,[5,24] maleimide−thiol chemistry,[25,26] and Cu(I) catalyzed click chemistry.[27]

While these methods have been used successfully in many instances, they typically suffer from significant background AuNP adsorption, wherein positively charged biomolecules readily adsorb to the negatively charged particles. This can be problematic for chemisorption, electrostatic adsorption, affinity-based noncovalent interactions, and some covalent conjugation strategies in which the AuNP surface is not passivated. In addition, AuNPs functionalized with *N*-hydroxysuccinimide (NHS) esters and maleimides are susceptible to hydrolysis in aqueous solutions, and the reported Cu(I)-mediated click strategy[27] suffers from extended reaction times (3 days). As a result, we sought to improve the existing bioconjugation strategies by adapting a previously reported oxidative coupling between anilines and *o*-aminophenols.[28,29] The reaction proceeds using potassium ferricyanide as a protein-tolerant oxidant in near neutral solutions (pH 6.5), and affords a single reaction product.[29] The involved precursors are stable in aqueous solutions, and the reaction proceeds quickly under mild conditions, allowing efficient coupling even at high dilution. As described herein, adapting this strategy for the bioconjugation of AuNPs has allowed us to overcome the limitations listed above to prepare functionalized particles for a wide variety of applications.

RESULTS AND DISCUSSION

To produce aniline-coated AuNPs that are stable in aqueous solutions, a AuNP surface passivating ligand was designed. As previous reports have shown a decrease in nonspecific adsorption of biomolecules to polyethylene glycol (PEG) coated AuNPs,[30] the ligand was based on a core PEG5k chain. The PEG5k was capped on one end with a disulfide to enable attachment to the AuNP surface, and terminated on the opposite end with an aniline moiety to allow for subsequent reactivity with *o*-aminophenols.

The AuNP modification strategy was based on compound **1** in Figure 1a. A straightforward synthesis was developed to prepare the desired ligand. Briefly, commercially available valeric acid-PEG5k-amine was reacted with the NHS ester of lipoic acid to afford valeric acid-PEG5k-lipoamide. The valeric acid terminus was then functionalized with 2-(4-aminophenyl)-ethylamine in the presence of NHS and *N*,*N*′-dicyclohexylcarbodiimide (DCC) to produce the desired aniline-PEG5k-lipoamide ligand. As a negative reaction control, a methoxy-PEG2k-lipoamide ligand, **2**, was synthesized in an analogous manner.

Received: August 12, 2014
Revised: September 17, 2014
Published: October 2, 2014

   dx.doi.org/10.1021/bc5003746 | *Bioconjugate Chem.* 2014, 25, 1888−1892

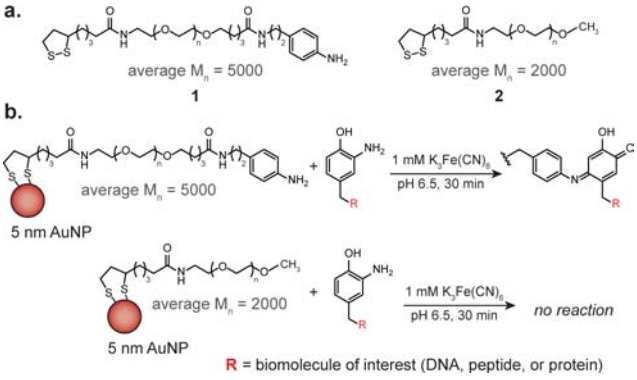

Figure 1. Strategy for the covalent attachment of biomolecules of interest to AuNPs (5 nm in diameter): (a) PEG-based nanoparticle passivating ligands were prepared with distal aniline (1) or methoxy (2) groups; (b) aniline-PEG5k-labeled AuNPs and *o*-aminophenol-containing DNA, peptides, or proteins were combined in the presence of potassium ferricyanide to afford stable conjugates. Methoxy-PEG2k-labeled AuNPs served as a control.

Overnight incubation of the aniline-PEG5k-lipoamide or methoxy-PEG2k-lipoamide with citrate-stabilized 5-nm-diameter AuNPs in a slightly basic solution (pH 8.5) afforded aniline- or methoxy-AuNPs, as shown in Figure 1b. The addition of the ligand was confirmed for both the aniline- and methoxy-coated AuNPs by an increase in the AuNP average diameter, as determined by dynamic light scattering (DLS, Supporting Information Figure S1) and a decrease in electrophoretic mobility of the AuNPs on a native agarose gel. The resulting particles were stable in solution for weeks, and resistant to precipitation at high salt concentrations (Supporting Information Figure S2).

As noted above, electrostatic attraction is often used to attach antibodies and other proteins to AuNPs. However, in other contexts these interactions render it difficult to attach biomolecules to specific sites. To evaluate nonspecific protein adsorption to the aniline-coated AuNPs and methoxy-coated AuNPs, which would impair our analysis of specific protein attachment, a selection of proteins (lysozyme, horseradish peroxidase, bacteriophage MS2, and bovine serum albumin) was incubated with bis(*p*-sulfonatophenyl)phosphine dehydrate dipotassium salt (BSPP) stabilized AuNPs, methoxy-coated AuNPs, and aniline-coated AuNPs overnight. Subsequent native agarose gel analysis allowed determination of nonspecific protein adsorption (Supporting Information Figure S3). Significant adsorption was observed for BSPP stabilized AuNPs with each of the proteins, but there was no observed protein adsorbed to the methoxy-AuNPs or aniline-AuNPs. With evidence that background adsorption would not be a major concern for the aniline-AuNPs or the control methoxy-AuNPs, the ability of these aniline-coated AuNPs to undergo oxidative coupling with *o*-aminophenol containing DNA, peptides, and proteins was evaluated.

Amine (5′) oligonucleotides were labeled with an *o*-nitrophenol NHS ester, followed by reduction with $Na_2S_2O_4$ to afford *o*-aminophenol DNA (Figure 2a). The sequences consisted of 7 nt (A), 14 nt (B), 16 nt (C), 20 nt (D, F, and F′), and 21 nt (E). The identity of these species was confirmed by MALDI-TOF MS (sequences A–F, Supporting Information Figure S4, S5). Reactions between *o*-aminophenol labeled oligonucleotides and aniline-AuNPs or the control methoxy-AuNPs were monitored by native agarose gel, as shown in

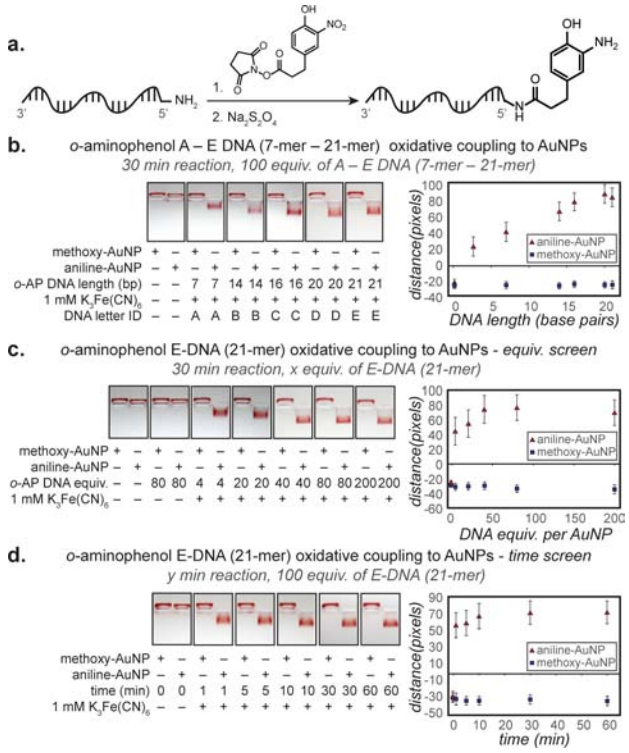

Figure 2. DNA attachment to aniline-AuNPs (5 nm in diameter). (a) Strategy for the introduction of an *o*-aminophenol to DNA sequences of interest. Amine (5′) oligonucleotides were labeled with an *o*-nitrophenol *N*-hydroxysuccinimide ester, followed by reduction with $Na_2S_2O_4$ to afford 5′-*o*-aminophenol DNA, as confirmed by MALDI-TOF MS (Supporting Information Figure S4). The electrophoretic mobility of the DNA-AuNP constructs was monitored by native agarose gel electrophoresis. The distance traveled toward the positive electrode (recorded as number of pixels from origin, 0 min = no addition of oxidant) was plotted for (b) varying lengths of DNA (7–21 bp), (c) DNA equivalents per AuNP (4–200 equiv), and (d) reaction time (0 to 60 min). Attachment of longer oligonucleotides resulted in a greater electrophoretic mobility of the DNA-AuNP conjugates. The maximum electrophoretic mobility of the conjugates was achieved at ∼40 equiv of DNA per AuNP and a 30 min reaction time. The vertical bars represent the width of each band, thus specifying a range of values.

Figure 2b–d. A gel shift was observed only for aniline-AuNPs in the presence of oxidant and an *o*-aminophenol labeled oligonucleotide. The distance traveled toward the positive electrode (recorded as the number of pixels from the origin in a digital photograph of the gel) was plotted for varying lengths of DNA (7–21 bp, Figure 2b), DNA equivalents per AuNP (4–200 equiv, Figure 2c), and reaction times (0 to 60 min, Figure 2d). The attachment of longer oligonucleotides resulted in a greater electrophoretic mobility of the DNA–AuNP conjugates, presumably due to an increase in negative charge on the AuNPs. The maximum electrophoretic mobility of the conjugates was achieved at ∼40 equiv of DNA per AuNP and a 30 min reaction time. Additionally, an increase in average particle diameter was observed for aniline-AuNPs coupled to *o*-aminophenol oligonucleotides in the presence of oxidant, as determined by DLS (Supporting Information Figure S1). The increase in average diameter indicated a high density of DNA strands on the AuNP surface. A similar size increase was not observed for the corresponding controls that were coated with

dx.doi.org/10.1021/bc5003746 | *Bioconjugate Chem.* 2014, 25, 1888–1892

methoxy-terminated PEG chains (Supporting Information Figure S1).

The ability of DNA labeled AuNPs to hybridize with complementary oligonucleotides was also evaluated. AuNPs were labeled with 20 nt sequence F, followed by incubation with its complement, F′ DNA. A slight increase in electrophoretic mobility was observed, as determined by native agarose gel (Supporting Information Figure S6). Analogous results were obtained when F′-coated AuNPs were incubated with sequence F. An increase in electrophoretic mobility was not observed upon incubating F-AuNPs or F′-AuNPs with noncomplementary oligonucleotides (Supporting Information Figure S6). Furthermore, incubation of F-AuNPs and F′-AuNPs in equal concentrations resulted in an increase in the overall average particle size in solution (as determined by DLS, Supporting Information Figure S1), indicating that the AuNPs labeled with complementary DNA are able to hybridize with each other to form large clusters in solution.

An *o*-aminophenol containing peptide was next tested for its attachment to aniline-AuNPs, as shown in Figure 3. A fibrin-

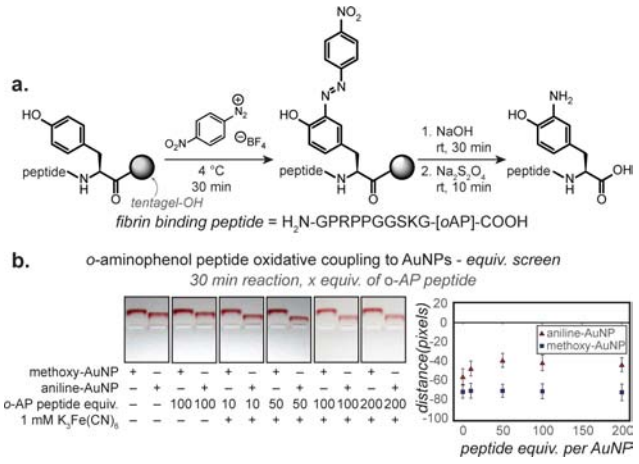

Figure 3. Peptide attachment to aniline-AuNPs (5 nm diameter). (a) Strategy for the introduction of an *o*-aminophenol on the fibrin-binding peptide, H_2N-GPRPPGGSKGY-COOH. The peptide was synthesied using standard solid-phase peptide synthesis chemistry. A C-terminal tyrosine residue was modified with 4-nitrobenzenediazonium tetrafluoroborate to afford the azo peptide, which was cleaved from the resin with base and reduced to the *o*-aminophenol with $Na_2S_2O_4$. Masses were confirmed by MALDI-TOF MS (Supporting Information Figure S7). (b) The electrophoretic mobility of the peptide-AuNP construct was monitored by native agarose gel electrophoresis. Distance traveled toward the positive electrode (recorded as number of pixels from origin) was plotted for increasing peptide equivalents per AuNP (10−200 equiv). The maximum electrophoretic mobility of the conjugates was achieved at ∼50 equiv peptide. All peptide-AuNP reactions proceeded at rt for 30 min. The vertical bars represent the width of each band, thus specifying the range of values.

binding peptide, H_2N-GPRPPGGSKGY-COOH,[31,32] was synthesized using standard solid-phase peptide synthesis chemistry on Tentagel-OH resin. Following side chain deprotection with TFA, the C-terminal tyrosine residue was modified with 4-nitrobenzenediazonium tetrafluoroborate to afford an azo peptide that was cleaved from the resin with base and reduced to the *o*-aminophenol with $Na_2S_2O_4$ (Figure 3a).[32] The molecular weights of these synthetic intermediates were confirmed by MALDI-TOF MS (Supporting Information Figure S7). The *o*-aminophenol terminated peptide was then coupled to aniline-AuNPs. The electrophoretic mobility of the peptide-AuNP construct was monitored by native agarose gel (Figure 3b). A change in mobility was observed only for the *o*-aminophenol peptide in the presence of aniline AuNPs and oxidant. The distance traveled toward the positive electrode (recorded as the number of pixels from the origin in a digital photograph of the gel) was plotted for increasing peptide equivalents per AuNP (10−200 equiv). All peptide coupling reactions proceeded at rt for 30 min. The maximum electrophoretic mobility of the conjugates was achieved at ∼50 equiv of peptide. An increase in average particle diameter was observed for the peptide-AuNP conjugates, as determined by DLS (Supporting Information Figure S1). The size increase indicated a high density of peptide coverage on the AuNP surface.

Next, *o*-aminophenol labeled proteins were tested for their attachment to aniline-AuNPs, as shown in Figure 4. Lysozyme, horseradish peroxidase, and bacteriophage MS2 were labeled with an *o*-nitrophenol NHS ester, as confirmed by ESI MS. For each protein, 1−3 modifications were observed (Supporting Information Figure S8). The *o*-nitrophenol groups were then reduced with $Na_2S_2O_4$ to afford *o*-aminophenol labeled lysozyme, horseradish peroxidase, and bacteriophage MS2 (Figure 4a).

The coupling reactions between *o*-aminophenol proteins and aniline- or methoxy-AuNPs were first monitored by native agarose gel electrophoresis. A minimal change in electrophoretic mobility was observed for the coupling of aniline AuNPs to *o*-aminophenol lysozyme (Figure 4b), while a clear change in electrophoretic mobility was visualized for both horseradish peroxidase and bacteriophage MS2 (Figure 4c,d). We attribute these differences to the number of equivalents used per AuNP in each reaction. Three, twenty, and ten equivalents of protein relative to AuNPs were used for the lysozyme, horseradish peroxidase, and bacteriophage MS2 coupling reactions, respectively. In the case of lysozyme, coupling reactions using more than 3 equiv of protein relative to AuNP resulted in conjugates that precipitated from solution. We attribute this instability to a significant change in surface charge and potential cross-linking between the particles. This possibility could be prevented using proteins bearing single *o*-aminophenol groups. Similar issues of conjugate instability were not observed in the case of horseradish peroxidase and bacteriophage MS2, allowing for greater equivalents to be used per reaction. The modest mobility shifts for lysozyme likely resulted from the small number of proteins on each particle.

As an additional characterization, the protein−AuNP conjugates were boiled in a solution of DTT and SDS (loading buffer) to reduce the AuNP-thiol bonds, affording the protein−polymer conjugate and precipitated gold aggregates (Figure 4b−d). This solution was then applied directly to an SDS-PAGE gel, revealing protein−polymer conjugates only when aniline-AuNPs were used. Consistent with the mobility experiments above, no protein−polymer conjugates were observed for the methoxy-AuNPs. In addition, the crude reaction mixture for lysozyme-AuNP and horseradish peroxidase-AuNP was subjected to 5−10 rounds of centrifugal filtration against 100 kDa MWCO filters to retain AuNP−protein conjugates and remove any unbound, unmodified protein. The removal of the unmodified protein was confirmed by SDS PAGE. To ensure that the protein−polymer conjugates

dx.doi.org/10.1021/bc5003746 | Bioconjugate Chem. 2014, 25, 1888−1892

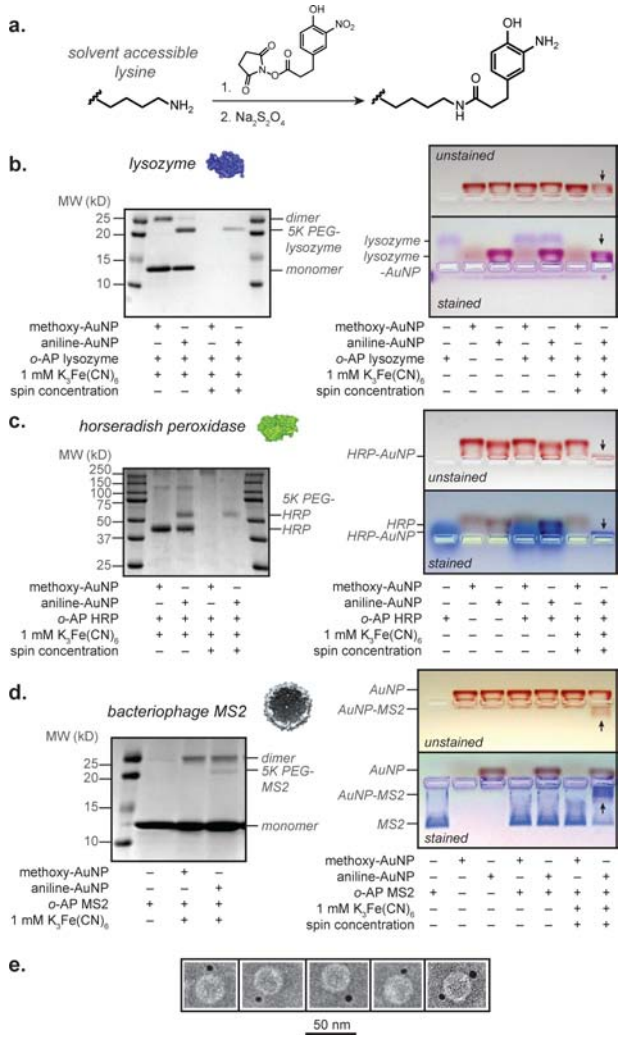

Figure 4. Protein attachment to aniline-AuNPs. (a) Strategy for the introduction of an *o*-aminophenol to proteins that contain solvent accessible lysine residues, including (b) lysozyme, (c) horseradish peroxidase, and (d) bacteriophage MS2. AuNP-protein conjugates had a slightly lower electrophoretic mobility than the corresponding controls when visualized by native agarose gel electrophoresis (right column, conjugate indicated by black arrow). PEG5k-protein conjugates were visualized through SDS PAGE gel electrophoresis (left column). Excess unmodified lysozyme and horseradish peroxidase were removed through successive centrifugal filtrations in 100 kDa MWCO filters. (e) MS2–AuNP conjugates were further characterized using TEM (scale bar = 50 nm).

were not simply retained in the 100 kDa MWCO filters due to their increase in hydrodynamic volume, lysozyme-PEG5k and horseradish peroxidase-PEG5k conjugates were independently synthesized and subjected to successive rounds of centrifugal filtration with 100 kDa MWCO filters. The protein–polymer conjugates were not retained in the filters (Supporting Information Figure S9), providing further support that the protein–polymer–AuNP conjugates were retained following successive rounds of centrifugal filtration only due to their attachment to the AuNPs. A similar strategy for removing unbound protein was not possible for bacteriophage MS2–AuNP conjugates because unmodified MS2 is retained by 100 kDa MWCO filters. Instead, the AuNP–MS2 conjugate was extracted from the native agarose gel and further characterized by transmission electron microscopy, revealing 1–2 AuNPs per capsid (Figure 4e; Supporting Information Figure S10).

CONCLUSIONS

This strategy presents a promising new method for the attachment of aniline-AuNPs to *o*-aminophenol-labeled biomolecules of interest. The reaction proceeds under mild conditions (pH 6.5, 1 mM oxidant) with fast reaction times (30 min) and little-to-no background protein adsorption to the AuNPs. In future experiments, we hope to use this strategy for the production of AuNP–biomolecule conjugates for imaging applications and for the immobilization of enzymes. We also plan to extend this method to include other thiophilic inorganic nanomaterials such as silver nanoparticles, CdSe/ZnS quantum dots, CdSe/CdS dot-rods, and certain Au-coated magnetic nanoparticles,[33] for the production of stable inorganic nanomaterial bioconjugates.

ASSOCIATED CONTENT

Supporting Information

Full experimental details, additional gel analysis, dynamic light scattering traces, transmission electron microscopy images, ^{1}H NMR, and mass spectrometry data. This material is available free of charge via the Internet at http://pubs.acs.org.

AUTHOR INFORMATION

Corresponding Author

*E-mail: mbfrancis@berkeley.edu. Tel: (510) 643-9915. Fax: (510) 643-3079.

Notes

The authors declare no competing financial interest.

ACKNOWLEDGMENTS

These studies were generously supported by the Director, Office of Science, Materials Sciences and Engineering Division, of the U.S. Department of Energy under Contract No. DEAC02-05CH11231. S.L.C. and A.C.O. were supported by NSF graduate research fellowships. A.M.E. was supported by the W.M. Keck Foundation. Transmission Electron Microscopy Images were obtained at the UC Berkeley Electron Microscope Lab.

REFERENCES

(1) Boisselier, E., and Astruc, D. (2009) Gold nanoparticles in nanomedicine: preparations, imaging, diagnostics, therapies and toxicity. *Chem. Soc. Rev. 38*, 1759–1782.

(2) Saha, K., Agasti, S. S., Kim, C., Li, X., and Rotello, V. M. (2012) Gold nanoparticles in chemical and biological sensing. *Chem. Rev. 112*, 2739–2779.

(3) Ghosh, P., Han, G., De, M., Kim, C. K., and Rotello, V. M. (2008) Gold nanoparticles in delivery applications. *Adv. Drug Delivery Rev. 60*, 1307–1315.

(4) Brennan, J. L., Kanaras, A. G., Nativo, P., Tshikhudo, T. R., Rees, C., Fernandez, L. C., Dirvianskyte, N., Razumas, V., Skjøt, M., Svendsen, A., Jørgensen, C. I., Schweins, R., Zackrisson, M., Nylander, T., Brust, M., and Barauskas, J. (2010) Enzymatic activity of lipase-nanoparticle conjugates and then digestion of lipid liquid crystalline assemblies. *Langmuir 26*, 13590–13599.

(5) Pandey, P., Singh, S. P., Arya, S. K., Gupta, V., Datta, M., Singh, S., and Malhotra, B. D. (2007) Application of thiolated gold nanoparticles for the enhancement of glucose oxidase activity. *Langmuir 23*, 3333–3337.

(6) Gole, A., Dash, C., Ramakrishnan, V., Sainkar, S. R., Mandale, A. B., Rao, M., and Sastry, M. (2001) Pepsin-gold colloid conjugates:

preparation, characterization, and enzymatic activity. *Langmuir 17*, 1674−1679.
(7) Mahmoud, K. A., Male, K. B., Hrapovic, S., and Luong, J. H. T. (2009) Cellulose nanocrystal/gold nanoparticle composite as a matrix for enzyme immobilization. *ACS Appl. Mater. Interfaces 1*, 1383−1386.
(8) Sperling, R. A., and Parak, W. J. (2010) Surface modification, functionalization and bioconjugation of colloidal inorganic nanoparticles. *Philos. Trans. R. Soc. London, Ser. A 368*, 1333−1383.
(9) Algar, W. R., Prasuhn, D. E., Stewart, M. H., Jennings, T. L., Blanco-Canosa, J. B., Dawson, P. E., and Medintz, I. L. (2011) The controlled display of biomolecules on nanoparticles: a challenge suited to bioorthogonal chemistry. *Bioconjugate Chem. 22*, 825−858.
(10) Rana, S., Yeh, Y.-C., and Rotello, V. M. (2010) Engineering the nanoparticle-protein interface: applications and possibilities. *Curr. Opin. Chem. Biol. 14*, 828−834.
(11) Ackerson, C. J., Powell, R. D., and Hainfeld, J. F. In *Methods in Enzymology* (Grant, J. J., Ed.) p 195, Vol. *481*, Academic Press, 2010 .
(12) Love, J. C., Estroff, L. A., Kriebel, J. K., Nuzzo, R. G., and Whitesides, G. M. (2005) Self-assembled monolayers of thiolates on metals as a form of nanotechnology. *Chem. Rev. 105*, 1103−1170.
(13) Lévy, R., Thanh, N. T. K., Doty, R. C., Hussain, I., Nichols, R. J., Schiffrin, D. J., Brust, M., and Fernig, D. G. (2004) Rational and combinatorial design of peptide capping ligands for gold nanoparticles. *J. Am. Chem. Soc. 126*, 10076−10084.
(14) Nativo, P., Prior, I. A., and Brust, M. (2008) Uptake and intracellular fate of surface-modified gold nanoparticles. *ACS Nano 2*, 1639−1644.
(15) Bastús, N. G., Sánchez-Tilló, E., Pujals, S., Farrera, C., López, C., Giralt, E., Celada, A., Lloberas, J., and Puntes, V. (2009) Homogeneous conjugation of peptides onto gold nanoparticles enhances macrophage response. *ACS Nano 3*, 1335−1344.
(16) Loweth, C. J., Caldwell, W. B., Peng, X., Alivisatos, A. P., and Schultz, P. G. (1999) DNA-based assembly of gold nanocrystals. *Angew. Chem., Int. Ed. 38*, 1808−1812.
(17) Ackerson, C. J., Jadzinsky, P. D., Jensen, G. J., and Kornberg, R. D. (2006) Rigid, specific, and discrete gold nanoparticle/antibody conjugates. *J. Am. Chem. Soc. 128*, 2635−2640.
(18) Aubin-Tam, M.-E., Hwang, W., and Hamad-Schifferli, K. (2009) Site-directed nanoparticle labeling of cytochrome c. *Proc. Natl. Acad. Sci. U.S.A. 106*, 4095−4100.
(19) Brewer, S. H., Glomm, W. R., Johnson, M. C., Knag, M. K., and Franzen, S. (2005) Probing BSA binding to citrate-coated gold nanoparticles and surfaces. *Langmuir 21*, 9303−9307.
(20) Geoghegan, W. D. (1988) The effect of three variables on adsorption of rabbit IgG to colloidal gold. *J. Histochem. Cytochem. 36*, 401−407.
(21) Peckys, D. B., Baudoin, J.-P., Eder, M., Werner, U., and de Jonge, N. (2013) Epidermal growth factor receptor subunit locations determined in hydrated cells with environmental scanning electron microscopy. *Nat. Sci. Rep. 3*, 1−6.
(22) Kogot, J. M., England, H. J., Strouse, G. F., and Logan, T. M. (2008) Single peptide assembly onto a 1.5 nm Au surface via a hidstidine tag. *J. Am. Chem. Soc. 130*, 16156−16157.
(23) Kogot, J. M., Parker, A. M., Lee, J., Blaber, M., Strouse, G. F., and Logan, T. M. (2009) Analysis of the dynamics of assembly and structural impact for a histidine tagged FGF1−1.5 nm Au nanoparticle bioconjugate. *Bioconjugate Chem. 20*, 2106−2113.
(24) Thi Ha Lien, N., Thi Huyen, L., Xuan Hoa, V., Viet Ha, C., Thanh Hai, N., Quang Huan, L., Emmanuel, F., Quang Hoa, D., and Hong Nhung, T. (2010) Synthesis, capping and binding of colloidal gold nanoparticles to proteins. *Adv. Nat. Sci.: Nanosci. Nanotechnol. 1*, 025009.
(25) Zhu, J., Waengler, C., Lennox, R. B., and Schirrmacher, R. (2012) Preparation of water-soluble maleimide- functionalized 3 nm gold nanoparticles: a new bioconjugation template. *Langmuir 28*, 5508−5512.
(26) Gobbo, P., and Workentin, M. S. (2012) Improved methodology for the preparation of water-soluble maleimide-functionalized small gold nanoparticles. *Langmuir 28*, 12357−12363.
(27) Brennan, J. L., Hatzakis, N. S., Tshikhudo, T. R., Razumas, V., Patkar, S., Vind, J., Svendsen, A., Nolte, R. J. M., Rowan, A. E., and Brust, M. (2006) Bionanoconjugation via click chemistry: the creation of functional hybrids of lipases and gold nanoparticles. *Bioconjugate Chem. 17*, 1373−1375.
(28) Behrens, C. R., Hooker, J. M., Obermeyer, A. C., Romanini, D. W., Katz, E. M., and Francis, M. B. (2011) Rapid chemoselective bioconjugation through the oxidative coupling of anilines and aminophenols. *J. Am. Chem. Soc. 133*, 16398−16401.
(29) Obermeyer, A. C., Jarman, J. B., Netirojjanakul, C., El Muslemany, K., and Francis, M. B. (2014) Mild bioconjugation through the oxidative coupling of *ortho*-aminophenols and anilines with ferricyanide. *Angew. Chem., Int. Ed. 53*, 1057−1061.
(30) Walkey, C. D., Olsen, J. B., Guo, H., Emili, A., and Chan, W. C. W. (2011) Nanoparticle size and surface chemistry determine serum protein adsorption and macrophage uptake. *J. Am. Chem. Soc. 134*, 2139−2147.
(31) Laudano, A. P., and Doolittle, R. F. (1978) Synthetic peptide derivatives that bind to fibrinogen and prevent polymerization of fibrin monomers. *Proc. Natl. Acad. Sci. U.S.A. 75*, 3085−3089.
(32) Obermeyer, A. C., Capehart, S. L., Jarman, J. B., and Francis, M. B. (2014) Multivalent viral capsids with internal cargo for fibrin imaging. *PLoS One 9*, e100678.
(33) Lyon, J. L., Fleming, D. A., Stone, M. B., Schiffer, P., and Williams, M. E. (2004) Synthesis of Fe oxide core/Au shell nanoparticles by iterative hydroxylamine seeding. *Nano Lett. 4*, 719−723.